Transition from Antibunching to Bunching in Cavity QED

Markus Hennrich,* Axel Kuhn, and Gerhard Rempe
Max-Planck-Institut für Quantenoptik, Hans-Kopfermann-Strasse 1, D-85748 Garching, Germany
(Received 4 June 2004; published 10 February 2005)

The photon statistics of the light emitted from an atomic ensemble into a single field mode of an optical cavity is investigated as a function of the number of atoms. The light is produced in a Raman transition driven by a pump laser and the cavity vacuum, and a recycling laser is employed to repeat this process continuously. For weak driving, a smooth transition from antibunching to bunching is found for about one intracavity atom. Remarkably, the bunching peak develops within the antibunching dip. The observed behavior is well explained by a model describing an ensemble of independent emitters.

DOI: 10.1103/PhysRevLett.94.053604 PACS numbers: 42.50.Dv, 42.50.Fx, 42.55.Ye, 42.65.Dr

The photon statistics of light reveals whether it originates from a classical or a quantum source like a single atom. These sources can be distinguished by their intensity correlation function, $g^{(2)}(\tau)$ [1]. Classical light fulfills the Cauchy-Schwarz inequality, $g^{(2)}(0) \geq g^{(2)}(\tau)$, whereas light that violates this inequality must be described by the laws of quantum physics. In this case, a local minimum at $\tau = 0$ is found, i.e. $g^{(2)}(0) < g^{(2)}(\tau)$, which is defined as antibunching [2]. First experiments demonstrating antibunching were performed with a weak beam of atoms [3]. Limitations imposed by number fluctuations [4] were later eliminated by using a single emitter [5–11]. The deterministic control of the nonclassical light radiated by a single emitter [12–18] has interesting applications, e.g., in quantum information processing. Classical bunching, $g^{(2)}(0) > g^{(2)}(\tau)$, has been observed in the fluorescence of a large number of independently radiating atoms as early as 1956 [19], and has regained new interest in the context of cold-atom physics [20,21].

A smooth transition between antibunching and bunching is expected if the number of atoms gradually increases. Such a transition has not been observed so far, since a good photon-collection efficiency, and thus a large solid angle, is essential to obtain a photon count rate large enough to discriminate the antibunching signal from background noise, while spatial coherence of the detected light is required to observe bunching. For a distributed ensemble of atoms, this calls for a small solid angle. Obviously, these two requirements contradict each other, making the experiment difficult in the interesting regime of just a few radiating particles.

In the work presented here, all emitters are coupled to a single mode in a high-finesse optical cavity. Only the light in this mode is investigated, so that spatial coherence is granted. At the same time, the enhanced spontaneous emission into the cavity mode gives a good photon-collection efficiency. The experiment is performed in a regime where an emitted photon leaves the cavity before being reabsorbed and before affecting other atoms. Vacuum-Rabi oscillations and collective effects are therefore largely suppressed. Moreover, the laser beams exciting the atoms are running perpendicular to the cavity axis, so that the photon statistics of the light emitted from the cavity is not the result of a driving field interfering with the atomic emission, as for an axially excited cavity [22–24]. It follows that all requirements to observe the transition between antibunching and bunching for independently fluorescing atoms with one-and-the-same experimental setup are fulfilled. In fact, we find that, with an increasing number of atoms, a strong bunching peak (demonstrating the wave character of the light) develops inside the antibunching minimum at $\tau = 0$ (characterizing the particle nature of the light).

Figure 1 illustrates the setup. A cloud of ^{85}Rb atoms released from a magneto-optical trap (MOT) falls through a 1 mm long optical cavity of finesse $F = 60\,000$. The average number of atoms simultaneously interacting with the cavity, $\bar{N}$, is freely adjustable by the loading time of the trap between $\bar{N} = 0$ and $\bar{N} \approx 140$. In the cavity, the atoms are exposed to two laser beams. The pump laser continu-

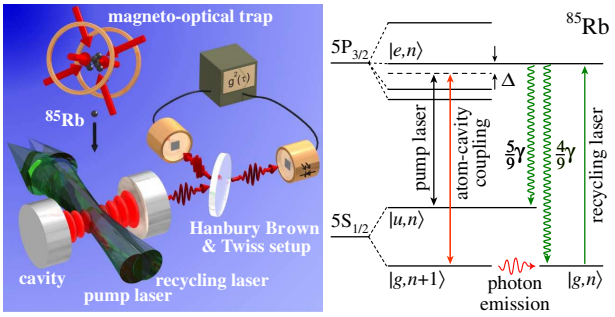

FIG. 1 (color online). Scheme of the experiment. Left: The setup shows that atoms are released from a magneto-optical trap and fall through a cavity 20 cm below with a velocity of 2 m/s. Each atom interacts with the TEM_{00} mode of the cavity for about 20 μs and is exposed to pump and recycling laser beams. The light emitted from the cavity is registered by a pair of photodiodes. Right: Relevant levels and transitions in ^{85}Rb. The atomic states $|u\rangle$, $|e\rangle$, and $|g\rangle$ are involved in the Raman process, and the states $|n\rangle$ and $|n+1\rangle$ denote the cavity's photon number.

ously drives the transition between the state $|u\rangle \equiv |5S_{1/2}(F=3)\rangle$ and the excited state $|e\rangle \equiv |5P_{3/2}(F=3)\rangle$ with Rabi frequency Ω_P, while the cavity couples $|e\rangle$ to the other hyperfine ground state, $|g\rangle \equiv |5S_{1/2}(F=2)\rangle$. Both fields are detuned by an amount Δ from the respective atomic transition so that they resonantly drive a Raman transition between $|u\rangle$ and $|g\rangle$ which also changes the intracavity photon number by one. At the same time, a recycling laser of Rabi frequency Ω_R resonantly drives the transition from $|g\rangle$ to $|e\rangle$, from where the atoms decay back to state $|u\rangle$. This closes the excitation loop and enables each atom to emit several photons on its way through the cavity. Because of the continuous driving, the Raman transitions are stochastic in contrast to the adiabatically driven Raman transition process reported in [15,25–27]. The dynamics of the system is determined by $(g_{\max}, \kappa, \gamma, \Omega_P, \Omega_R, \Delta) = 2\pi \times (2.5, 1.25, 3.0, 7.6, 3.3, -20)$ MHz, where $g_{\max}$ is the cavity-induced coupling between states $|e,0\rangle$ and $|g,1\rangle$ for an atom optimally coupled to the cavity, and κ and γ are the field and polarization decay rates of the cavity and the atom, respectively. The maximum recycling rate is achieved when the transition between $|g\rangle$ and $|e\rangle$ is strongly saturated. In this case, both levels are equally populated leading to a recycling rate of $R_{\max} = \frac{5}{9}\gamma = 2\pi \times 1.7$ MHz, where $\frac{5}{9}$ is the average branching ratio for a decay from $|e\rangle$ to $|u\rangle$. Therefore the recycling is always slower than the decay of the cavity excitation, 2κ. For the above value of Ω_R, the recycling is about 4 times slower than the cavity decay, so that the cavity returns to the vacuum state before the next photon is placed into its mode from the same atom. Therefore nonclassical antibunching can be observed. The maximum effective Rabi frequency of the Raman process, $\Omega_{\text{eff}} = g_{\max}\Omega_P/\Delta = 2\pi \times 0.95$ MHz, is also smaller than the cavity decay rate. Therefore the system is overdamped and shows no Rabi oscillations; i.e., both the reabsorption of emitted photons and the cavity-mediated interaction between different atoms are negligible. The cavity decay is mainly caused by the 100 ppm transmittance of one of the mirrors. Photons leave the cavity through this output coupler with a probability of 90%, and are detected by two photodiodes with 50% quantum efficiency that are placed at the output ports of a beam splitter. They form a Hanbury Brown and Twiss setup to measure the $g^{(2)}(\tau)$ intensity correlation function of the light. To avoid a limitation to a waiting-time distribution between successive photons, all photodetection times are registered and taken into account in the evaluation.

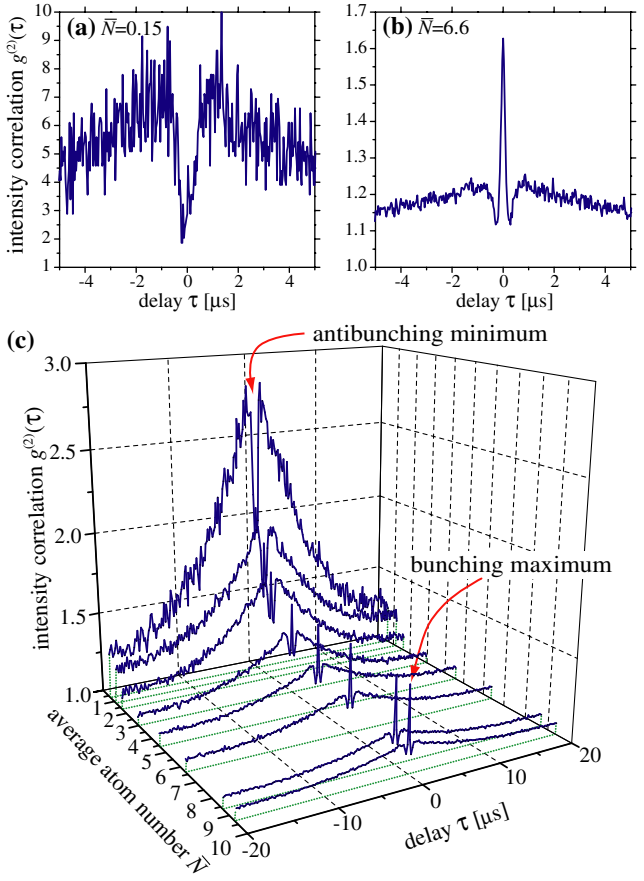

FIG. 2 (color online). Intensity correlation, $g^{(2)}(\tau)$, as a function of the detection time delay, τ, for different values of the average atom number, $\bar{N}$. A transition from antibunching to bunching is observed for $\bar{N} \approx 1$. To adjust $\bar{N}$, we load the trap between 20 ms and 2.5 s. For each trace, we load and release atoms from the MOT 500 times and register photons during $\delta t =$ 8 ms while the atom cloud traverses the cavity.

Figure 2 shows $g^{(2)}(\tau)$ for different settings of the atom flux. For an average atom number below one, $\bar{N} = 0.15$, it shows nonclassical antibunching, i.e., a local minimum at $\tau = 0$ in Fig. 2(a). Note that sub-Poissonian light with $g^{(2)}(0) < 1$ is not observed because the Poissonian statistics of the atomic cloud is mapped to the photon statistics. When the atom flux is increased to $\bar{N} > 1$, a transition to bunching, i.e., a local maximum at $\tau = 0$, is observed; see Figs. 2(b) and 2(c).

This transition from nonclassical light for $\bar{N} < 1$ to classical light for $\bar{N} > 1$ can be explained with a model [4] that describes an ensemble of independent emitters where the electric field of all atoms,

$$E(t) = \sum_{i=1}^{N(t)} E_i(t), \tag{1}$$

is the sum of the fields radiated by the individual atoms, $E_i(t)$. Obviously, the individual fields interfere with the fields radiated by the other atoms. For independent emitters, correlations between the fields of different atoms can be neglected. Following [4] and provided the atom distribution is Poissonian with an average atom number $\bar{N}$ [28], the intensity correlation function reads

$$g^{(2)}(\tau) = 1 + |f(\tau)g_A^{(1)}(\tau)|^2 + f(\tau)g_A^{(2)}(\tau)/\bar{N}. \tag{2}$$

It consists of three different contributions: (i) The constant term 1 stems from photons that are independently emitted by different atoms, i.e., it reflects the atom statistics which is directly mapped to the light. (ii) The bunching term, $|f(\tau)g_A^{(1)}(\tau)|^2$, with $g_A^{(1)}(\tau)$ the autocorrelation function of the electric field emitted by one atom and $f(\tau)$ given below [29], results from the beating of the light emitted by different atoms. Constructive or destructive interference leads to a fluctuating intensity [1]. If a photon is detected, constructive interference is likely and the probability for a second photodetection is increased. The opposite holds for destructive interference. The interference and the correlated behavior vanish if the two photodetections are separated by more than the coherence time. Therefore the bunching contribution decreases with the square of $g_A^{(1)}(\tau)$, whose $\frac{1}{e}$ decay defines the coherence time, τ_c. Note that this contribution does not depend on the number of atoms and therefore persists for very high atom flux. (iii) The antibunching term, $f(\tau)g_A^{(2)}(\tau)/\bar{N}$, with $g_A^{(2)}(\tau)$ the single-atom intensity correlation function, is attributed to the photons emitted from an individual atom. After a photon emission, the atom must be recycled to state $|u\rangle$ before it can emit another photon. This leads to antibunching. Because of the statistical nature of the recycling, photons are uncorrelated for large $|\tau|$, and $g_A^{(2)}(\tau \to \pm\infty)$ reaches 1. However, only photons emitted from one-and-the-same atom during its limited interaction time with the cavity contribute. The envelope function, $f(\tau)$, with $f(\tau \to \pm\infty) = 0$, takes this into account. Note that the antibunching term scales with the inverse average atom number, $1/\bar{N}$, and therefore vanishes for large $\bar{N}$.

The three contributions explain the observed transition from antibunching to bunching shown in Fig. 2(c): the antibunching contribution for $\bar{N} < 1$ vanishes with increasing atom number while the bunching contribution does not change. For a detailed comparison of this model with the experiment, we write the correlation function as $g^{(2)}(\tau, 1/\bar{N}) = A(\tau) + B(\tau)/\bar{N}$, with

$$|g_A^{(1)}(\tau)|^2 = \frac{A(\tau) - 1}{f^2(\tau)}, \qquad g_A^{(2)}(\tau) = \frac{B(\tau)}{f(\tau)}. \tag{3}$$

For every value of τ, we can now obtain $A(\tau)$ and $B(\tau)$ from a linear fit to the experimentally observed $g^{(2)}(\tau, 1/\bar{N})$ as a function of $1/\bar{N}$ [30]. For the two examples $\tau = 0$ and $\tau = 1$ μs, Fig. 3(a) shows that this procedure is indeed justified, as the experimental data show a linear dependence on $1/\bar{N}$. The same result holds for other values of τ. The offset $A(\tau) = \lim_{\bar{N}\to\infty} g^{(2)}(\tau, 1/\bar{N})$ represents the two $\bar{N}$-independent contributions, (i) and (ii), from above, whereas the slope $B(\tau) = d(g^{(2)}(\tau, 1/\bar{N}))/d(1/\bar{N})$ determines the size of the antibunching contribution. A decomposition of $g^{(2)}(\tau, 1/\bar{N})$ into these contributions is shown in Fig. 3(b). $A(\tau)$ consists of the constant term 1 plus the bunching peak, whereas $B(\tau)$ shows an antibunching dip and decays with an envelope function $f(\tau)$ that is imposed by the atom transit.

Figure 4 shows the single-atom correlation functions deduced from $A(\tau)$ and $B(\tau)$ using the relations (3). These functions reveal the relevant experimental time scales. The minimum delay between two successive photons from one-and-the-same atom corresponds to the $1/e$ half width of the antibunching dip, $\tau_A = 430 \pm 10$ ns. This is much larger than the photon lifetime in the cavity, $\kappa^{-1}/2 = 64$ ns, so that successive photons from a single atom hardly overlap. From the decay of the field correlation function, $|g_A^{(1)}(\tau)|^2$, we calculate a coherence time of the emitted light of $\tau_c = 170 \pm 2$ ns (half $1/e^2$ width), larger than the decay time of the cavity field, $\kappa^{-1} = 128$ ns. This seemingly unexpected result is not surprising as the coherence properties are controlled by the photon-

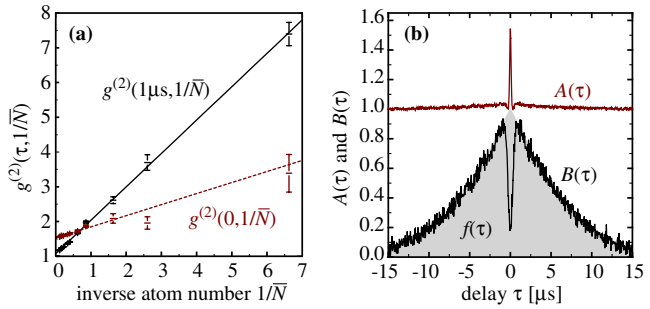

FIG. 3 (color online). (a) Decomposition of $g^{(2)}(\tau, 1/\bar{N})$: Linear-regression fit as a function of $1/\bar{N}$ for $\tau = 0$ and $\tau = 1$ μs. For each τ, the offset $A(\tau)$ and the slope $B(\tau)$ are obtained from such fits. (b) Bunching and antibunching contributions, $A(\tau)$ and $B(\tau)$, respectively. Modeling $B(\tau)$ for $|\tau| > 1.0$ μs yields the empirical envelope, $f(\tau) = \exp(-|\tau/6.5\ \mu s|^{1.22})$ (shaded).

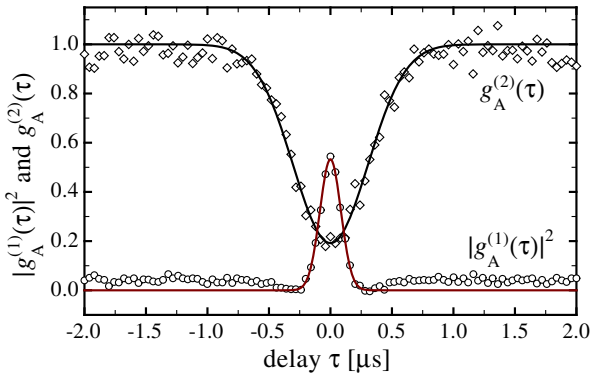

FIG. 4 (color online). Single-atom correlations, $|g_A^{(1)}(\tau)|^2$ and $g_A^{(2)}(\tau)$, deduced from $A(\tau)$, $B(\tau)$, and $f(\tau)$ using Eq. (3). The two contributions weighted according to Eq. (2) determine the observed photon statistics, $g^{(2)}(\tau)$, as shown in Fig. 2. Because of a small cross talk between $g_A^{(2)}(\tau)$ and $|g_A^{(1)}(\tau)|^2$, the latter stays larger than zero for values of τ smaller than the atom-cavity interaction time.

generating Raman process, which takes longer than the cavity decay time [31]. We also note that the peak amplitude of the field correlation function, $|g_A^{(1)}(0)|^2 = 0.53 \pm 0.01$, is very close to the expectation value for independently emitting atoms, which is $|g_A^{(1)}(0)|^2 = 0.5$ for unpolarized light [32].

The only small discrepancy from our expectations is that $g_A^{(2)}(\tau = 0)$ does not vanish completely as one would expect for the resonance fluorescence of single atoms [33]. Instead, we obtain $g_A^{(2)}(0) = 0.19 \pm 0.02$. This slight departure from perfect antibunching indicates that some atoms emit a second photon before the first photon has left the cavity. To assure that such collective effects do not dominate, we have verified that the photon number increases linearly with the average atom number in our parameter regime. Only with at least 100 atoms and drive Rabi frequencies raised by a factor of 3, does the average photon number show a slightly nonlinear increase with $\bar{N}$; i.e., a moderate amplification is found. However, no kink in the photon number is observed that would signal a lasing threshold. In fact, laser operation relies on a recycling rate much larger than the cavity decay rate, so that the photons remain long enough in the cavity to stimulate further emissions.

In conclusion, we have observed the transition from antibunching to bunching in the fluorescence light emitted from a high-finesse cavity with an increasing average number of atoms in the cavity. The cavity decay determines the fastest time scale, so that the atoms act as independent emitters. The agreement of our data with the predicted scaling behavior of the photon statistics is excellent, so that the single-atom correlation functions for antibunching and bunching, $g_A^{(2)}(\tau)$ and $g_A^{(1)}(\tau)$, respectively, can be extracted. It would be interesting to apply a similar analysis to a lasing atom-cavity system [7], where cooperative effects are expected to dominate the photon statistics.

We thank B. W. Shore for stimulating discussions. This work was supported by the Deutsche Forschungsgemeinschaft (SPP 1078 and SFB 631) and the European Union [IST (QGATES) and IHP (CONQUEST) programs].

*Present address: ICFO–Institut de Ciències Fotòniques, Jordi Girona 29, Nexus II, 08034 Barcelona, Spain.

[1] M. O. Scully and M. Zubairy, *Quantum Optics* (Cambridge University Press, Cambridge, U.K., 1997).
[2] L. Mandel and E. Wolf, *Optical Coherence and Quantum Optics* (Cambridge University Press, Cambridge, U.K., 1995), Chap. 14.7.3.
[3] H. J. Kimble, M. Dagenais, and L. Mandel, Phys. Rev. Lett. **39**, 691 (1977).
[4] H. J. Carmichael, P. Drummond, P. Meystre, and D. F. Walls, J. Phys. A **11**, L121 (1978).
[5] F. Diedrich and H. Walther, Phys. Rev. Lett. **58**, 203 (1987).
[6] V. Gomer, F. Strauch, B. Ueberholz, S. Knappe, and D. Meschede, Phys. Rev. A **58**, R1657 (1998).
[7] J. McKeever, A. Boca, A. D. Boozer, J. R. Buck, and H. J. Kimble, Nature (London) **425**, 268 (2003).
[8] F. De Martini, G. Di Giuseppe, and M. Marrocco, Phys. Rev. Lett. **76**, 900 (1996).
[9] P. Michler *et al.*, Nature (London) **406**, 968 (2000).
[10] C. Kurtsiefer, S. Mayer, P. Zarda, and H. Weinfurter, Phys. Rev. Lett. **85**, 290 (2000).
[11] A. Beveratos, R. Brouri, T. Gacoin, J.-P. Poizat, and P. Grangier, Phys. Rev. A **64**, 061802 (2001).
[12] B. Lounis and W. E. Moerner, Nature (London) **407**, 491 (2000).
[13] P. Michler *et al.*, Science **290**, 2282 (2000).
[14] C. Santori, D. Fattal, J. Vučković, G. S. Solomon, and Y. Yamamoto, Nature (London) **419**, 594 (2002).
[15] A. Kuhn, M. Hennrich, and G. Rempe, Phys. Rev. Lett. **89**, 067901 (2002).
[16] A. Beveratos *et al.*, Phys. Rev. Lett. **89**, 187901 (2002).
[17] J. McKeever *et al.*, Science **303**, 1992 (2004).
[18] M. Keller, B. Lange, K. Hayasaka, W. Lange, and H. Walther, Nature (London) **431**, 1075 (2004).
[19] R. Hanbury Brown and R. Q. Twiss, Nature (London) **178**, 1046 (1956).
[20] C. Jurczak *et al.*, Phys. Rev. Lett. **77**, 1727 (1996).
[21] S. Bali, D. Hoffmann, J. Simán, and T. Walker, Phys. Rev. A **53**, 3469 (1996).
[22] J. Carmichael, R. J. Brecha, and P. R. Rice, Opt. Commun. **82**, 73 (1991).
[23] G. Rempe, R. J. Thompson, R. J. Brecha, W. D. Lee, and H. J. Kimble, Phys. Rev. Lett. **67**, 1727 (1991).
[24] S. L. Mielke, G. T. Foster, and L. A. Orozco, Phys. Rev. Lett. **80**, 3948 (1998).
[25] M. Hennrich, T. Legero, A. Kuhn, and G. Rempe, Phys. Rev. Lett. **85**, 4872 (2000).
[26] A. Kuhn and G. Rempe, in *Experimental Quantum Computation and Information*, edited by F. De Martini and C. Monroe (IOS Press, Amsterdam, 2002), Vol. 148, pp. 37–66.
[27] M. Hennrich, A. Kuhn, and G. Rempe, J. Mod. Opt. **50**, 935 (2003).
[28] For $\tau \geq 1$ μs, we assume that $g_A^{(2)} = 1$ and $g_A^{(1)} \approx 0$. With $f(1\ \mu\text{s}) \approx 1$, this leads to $g^{(2)}(1\ \mu\text{s}, \bar{N} = 1) \approx 2$. This value is used to calibrate the atom flux leading to $\bar{N} = 1$. Relative to this calibration, $\bar{N}$ is then adjusted by laser-induced fluorescence.
[29] H. J. Kimble, M. Dagenais, and L. Mandel, Phys. Rev. A **18**, 201 (1978).
[30] Variations of the atom density lead to a small modulation of $g^{(2)}(\tau)$ in the millisecond regime. This contribution was subtracted to prevent a falsification of the fit.
[31] T. Legero, T. Wilk, M. Hennrich, G. Rempe, and A. Kuhn, Phys. Rev. Lett. **93**, 070503 (2004).
[32] With $|g_A^{(1)}(0)|^2 = 1$ for each polarization mode, and uncorrelated orthogonal modes (in both ways), the average of these four contributions leads to $|g_A^{(1)}(0)|^2 = 0.5$.
[33] H. J. Carmichael and D. F. Walls, J. Phys. B **9**, 1199 (1976).